Special Issue Article

Institution of MECHANICAL ENGINEERS
Journal of RISK AND RELIABILITY

Proc IMechE Part O:
J Risk and Reliability
2018, Vol. 232(2) 216–224

DOI: 10.1177/1748006X17744382
journals.sagepub.com/home/pio
SAGE

Modeling an electric power microgrid by model predictive control for analyzing its characteristics from reliability, controllability and topological perspectives

Fangyuan Han[1] and Enrico Zio[1,2]

Abstract

Microgrids can be a key solution for integrating renewable and distributed energy resources. This article analyzes microgrids' characteristics adopting model predictive control. We study the microgrid performance under two operation modes: grid-connected and stand-alone. For each mode, we consider different faulty scenarios, and by dynamic simulations, we investigate the importance of the microgrid components from different perspectives: topological, reliability and controllability. This analysis enables evaluation of the microgrid performance and quantification of the importance of each component with respect to the different perspectives considered. The findings provide information for the design and operation of a microgrid, seeking the right balance of multiple characteristics.

Keywords

Microgrid modeling, model predictive control, reliability, controllability, network topology

Date received: 8 September 2016; accepted: 28 October 2017

Introduction

Critical infrastructures, like electricity or gas transmission and distribution systems, rail and road transport or communication networks, are essential to the functioning of modern society.[1] They are designed to perform reliably and safely for long periods of times.[2,3] The complexity of these systems calls for new approaches of analysis, and a framework is needed to integrate a number of methods capable of viewing the problem from different perspectives.[4–6] Integration of different perspectives has been sought. For example, in Zio and Golea,[7] an electrical transmission system is analyzed with the objective of identifying the most critical elements in terms of four different perspectives; in Li et al.,[8] the correlation between connectivity reliability and controllability of network systems has been studied and in Zhang et al.,[9] the authors perform network reliability analysis considering spatial constraints.

In this article, we focus on power distribution systems and distributed generation, and in particular, microgrids which offer an interesting solution for integrating renewable and distributed energy resources. A microgrid is a cluster of micro-sources, storage systems and loads, which can be connected to the power grid as a single entity that can respond to central control signals.[10] The control problem for this kind of systems is particularly difficult as it is necessary to consider both exogenous factors (e.g. variations of wind speed and consumer demand) and the structural properties and internal dynamics of individual components (e.g. links and storage devices), which may change due to degradation, failure and other factor.[11] Various approaches for control and energy management of microgrids are reported in the literature.[12] In previous studies,[13–16] an agent-based modeling approach is proposed to model microgrids and to analyze by simulation the interactions between individual intelligent decision-makers.

[1]Chair on Systems Science and the Energy Challenge, Fondation EDF, CentraleSupelec, Gif-sur-Yvette, France
[2]Department of Energy, Politecnico di Milano, Milano, Italy

Corresponding author:
Enrico Zio, Chair on Systems Science and the Energy Challenge, Fondation EDF, CentraleSupelec, Bâtiment Francis Bouygues, 9 rue Joliot-Curie, 91190, Gif-sur-Yvette, France.
Email: enrico.zio@centralesupelec.fr

Han et al.[11] and Prodan and Zio[17,18] develop an optimization-based control approach.

It is considered that microgrids can improve the reliability of servicing local loads,[19,20] besides that of the power grid to which they are connected. In this work, we consider a microgrid system and adopt a graph representation and dynamic modeling for capturing its structural properties and internal dynamics. Different perspectives are considered for the analysis of the system topology, reliability and controllability.

Model predictive control (MPC),[21,22] a widely used technique in the control community, can be used to manage the dynamics of systems affected by uncertainties in the behavior of their components.[11] It is able to handle control and state constraints, while offering good control performance. For this, in MPC, the objective (or cost) function is constructed to penalize deviations of the states and inputs from their reference values, while the constraints are enforced explicitly.[23] Recently, MPC has been considered for refrigeration systems,[24] heating systems,[25] power production plants[26] and transportation networks.[27]

In this article, the MPC framework is proposed to analyze the microgrid under various faulty scenarios.

The original contributions are the following:

- The formulation of an optimization-based MPC problem for safety and reliability considerations of microgrid systems.
- The development and application of a simulation-based scheme for the analysis of a microgrid from different perspectives: reliability, controllability and topology.

The remainder of the article is organized as follows. Section "System modeling and description" describes in detail the representation of the microgrid system, including its network representation, the dynamic model, and the formulation of the optimization-based control problem. In section "System property indexes," three system indicators are presented from different perspectives. Section "Case study and simulation results" presents simulation results for different faulty scenarios. Finally, conclusions are drawn in section "Conclusion."

System modeling and description

Graph representation of the microgrid

Graph theory provides a natural framework for the mathematical representation of complex networks.[28,29] A graph is an ordered pair $\mathbf{G}(V, E)$ comprising a set of nodes (vertices) $V = v_1, v_2, \ldots, v_n$ together with a set of links (also called edges or arcs) $E = e_1, e_2, \ldots, e_m$, which are two-element subsets of V. The topological structure of a microgrid can be represented by a directed graph: the nodes represent the components or subsystems of the microgrid and the directional edges represent the functional links between the microgrid components.

The network structure is usually defined by the $n \times n$ adjacency matrix $\mathbf{A}$, which can be constructed as follows: if there is an edge from node i to node j, then we put a value of 1 in the entry on row i and column j of the matrix; otherwise, we put a value of 0. The $n \times n$ capacity matrix $\mathbf{K}$ contains information about the capacity constraints of the links.

Dynamic modeling of the microgrid

We introduce the dynamic model for representing the characteristics of the nodes and the flow in the links of the microgrid. We adopt a state-space model based on differential equations to describe the response of the system states to operational and environmental changes. The dynamics of the system is described by the following linear time-invariant equations

$$\begin{aligned} \mathbf{x}(t+1) &= \mathbf{A}\mathbf{x}(t) + \mathbf{B}\mathbf{u}(t) \\ \mathbf{y}(t) &= \mathbf{C}\mathbf{x}(t) + \mathbf{D}\mathbf{u}(t) \end{aligned} \tag{1}$$

where $\mathbf{x}$ is the state vector, $\mathbf{u}$ is the vector of control input, and $\mathbf{y}$ is the output vector. $\mathbf{A}$, $\mathbf{B}$, $\mathbf{C}$ and $\mathbf{D}$ are state transition matrices.

The components of the microgrid can be divided into different groups according to their functionalities: links, storage devices, suppliers (renewable generators), transporters, and consumers. The state vector $\mathbf{x}$ represents mainly the states of the links and storages devices, which are treated as dynamic, whereas the states of other nodes are considered static.

Link dynamics. For a link l_i, the state $x_{l_i}(t)$ indicates the capacity of the link to deliver power from one component to the other connected one at time t. It is assumed to be determined by both the input flow and the state of the previous time step. Its dynamic can be described as follows

$$x_{l_i}(t+1) = (1-\alpha_i)x_{l_i}(t) + \alpha_i \sum\nolimits_{l_{in} \in I_{l_i}} u_{l_{in}}(t) \tag{2}$$

where α_i is a coefficient of small value characterizing the inertia of flow transmission that depends on the physical characteristics of the link l_i, $u_{l_{in}}(t)$ is an input flow of the link l_i, and I_{l_i} is the set of input flows of the the link l_i.

Storage device dynamics. For a storage device s_i, its state $x_{s_i}(t)$ represents the energy storage level at time step t and depends on the energy level of the previous time step and the charge or discharge rates. The dynamic is described as

$$x_{s_i}(t+1) = (1-\tau_i)x_{s_i}(t) + \sum_{s_{in} \in I_{s_i}} u_{s_{in}}(t) - \sum_{s_{out} \in O_{s_i}} u_{s_{out}}(t) \tag{3}$$

with the mixed-integer conditions[17]

$$\begin{cases} 0 \leqslant \sum u(t) \leqslant Ma(t) \\ 0 \leqslant \sum x(t) \leqslant M(1 - a(t)) \end{cases} \quad (4)$$

where τ denotes the hourly self-discharge decay. $u_{s_{in}}(t)$ and $u_{s_{out}}(t)$ are input and output flow of the storage device s_i, respectively, and I_{s_i} and O_{s_i} are the sets of input and output flows of the storage device s_i, respectively. M represents a constraint and $a(t) \in \{0, 1\}$ is an auxiliary binary variable, characterizing the battery state of charge: when $a(t) = 1$ the battery is in discharge mode and when $a(t) = 0$ the battery is in charge mode.[11]

Optimization-based control for system safety analysis

The microgrid safety performance measured in terms of satisfaction of consumer power demands and solves an optimization problem in order to find the control input that minimizes the cost function $Cost(t)$ (e.g. the difference between the power demanded by the consumer and that actually received), which subject to a set of system constraints considering predicted profiles

$$\min_{[\mathbf{u}(t)]_{t=k:k+N_p}} \sum_{t=k}^{k+N_p} Cost(t)$$

Constraints on sources (renewable generators). Renewable generators are considered as the source of flows in a microgrid. Therefore, the total amount of output flows of a supplier p_i should be lower than its supply capacity

$$\sum_{p_{out} \in O_{p_i}} u_{p_{out}}(t) \leqslant K_{p_i} \quad (5)$$

where $u_{p_{out}}(t)$ is an output flow of the source p_i, O_{p_i} is the set of output flows of the source p_i, and K_{p_i} is the capacity of of the source p_i.

Constraints on transporters. A transporter t_i is a static node related to transmission or distribution, where the dynamic flows follow basic conservation laws, that is, the total amount of the output flows is equal to that of the input flows

$$\sum_{t_{in} \in I_{t_i}} u_{t_{in}}(t) = \sum_{t_{out} \in O_{t_i}} u_{t_{out}}(t) \quad (6)$$

where $u_{t_{in}}(t)$ and $u_{t_{out}}(t)$ are input and output flows of the transporter t_i, respectively, and I_{t_i} and O_{t_i} are the sets of input and output flows of the transporter t_i.

Constraints on consumers. The objective of the microgrid system is to supply power to satisfy consumer demand. Then, the amount of flows received by the consumer never exceeds its demand

$$y_{m_i} \leqslant D_{m_i}(t) \quad (7)$$

where $y_{m_i}(t)$ is the output of the system corresponding to the state of the consumer m_i and D_{m_i} is the demand of the consumer m_i.

Constraints on links. The flow through the link l_i is constrained by its maximum capacity K_{l_i}

$$0 \leqslant x_{l_i} \leqslant K_{l_i} \quad (8)$$

where K_{l_i} is the maximum capacity of the link l_i.

Constraints on storage devices. The amount of flow charged in a storage device s_i is limited by its storage capacity S_{max_i} and by its base storage S_{min_i}

$$S_{min_i} \leqslant x_{s_i}(t) \leqslant S_{max_i} \quad (9)$$

Similar constraints apply to the rates of the battery charge

$$Sr_{min_i} \leqslant \Delta x_{s_i}(t) \leqslant Sr_{max_i} \quad (10)$$

System property indexes

Non-supplied demand

Microgids have been proposed to improve reliability and stability of electrical systems and to ensure power quality of modern grids and have the responsibility to ensure the supply to the essential loads.[12] Supply performance is a fundamental functional requirement for the microgrid. In this article, we call the system "safe" if it ensures the satisfaction of the consumers' essential demands. We introduce the non-supplied demand (NSD) as a measure of the network's capacity to satisfy its users' demands. The normalized NSD is introduced as a system-level index

$$NSD = 1 - \frac{\sum_{i}^{i=N_m} \omega_i y_{m_i}}{\sum_{i}^{i=N_m} \omega_i D_{m_i}} \quad (11)$$

where ω_i is the weight of the ith of the N_m users, y_{m_i} is the supply to user i, and D_{m_i} is its demand, which is considered as the target supply to user i. Then, the second term in equation (11) represents the satisfied proportion of users' demands. Since $y_{m_i} \leqslant D_{m_i}$, the index NSD is normalized to take values in $[0, 1]$. NSD equals 0 when the users' demands are fully supplied.

Controllability index

A dynamic system is controllable if, with a suitable choice of inputs, it can be driven from any initial state to any desired final state within finite time.[30] Taking a system safety perspective, controllability is the ability to guide the system behavior toward a safe state through the appropriate manipulation of a few input variables.[11,31]

From control theory, the system (as described by equation (1)) is controllable if and only if its controllability matrix has full rank[32]

$$rank\left[B\ AB \ldots A^{n-1}B\right] = n$$

where n is the number of state variables of the system. This criteria is called Kalman's controllability rank condition. The rank of the controllability matrix provides the dimension of the controllable subspace of the system.

In this work, the controllability index CI measures the controllable proportion of a dynamic system. It is defined as the ratio of the rank of the controllable subsystem to the rank of the system

$$CI = \frac{R_C}{n} \tag{12}$$

where $R_C = rank[B\ AB \ldots A^{n-1}B]$.

System capacity efficiency

We introduce the system capacity efficiency to measure how much flow the system topology allows to exchange. The capacity of flow exchange from nodes i to j through a path is determined by the capacity of the widest-capacity path between them, k_{ij}, which is the minimum-edge capacity in the path between the two nodes maximizing the capacity of the minimum-capacity edge. Then, the capacity efficiency of the whole system E_c is given by

$$E_C[\mathbf{G}] = \frac{1}{N(N-1)} \sum_{i \neq j \in \mathbf{G}} k_{ij} \tag{13}$$

The source-terminal capacity efficiency E_c^{st}, which only takes into account the transmission capacity between a source node and a terminal (demand) node, is given by

$$E_C^{st}[\mathbf{G}] = \frac{1}{N_{st}} \sum_{s \in \mathbf{S},\, t \in \mathbf{T}} c_{st} \tag{14}$$

Then, we define the source-terminal capacity efficiency index (EI^{st}) as the normalized E_C^{st}

$$EI^{st}[\mathbf{G}'] = \frac{E_C^{st}[\mathbf{G}']}{E_C^{st}[\mathbf{G}]} \tag{15}$$

where $\mathbf{G}'$ is the graph obtained by the removal of certain components from $\mathbf{G}$.

Case study and simulation results

Case study: microgrid

We consider the microgrid system in Figure 1, which is adopted from Han et al.[11] This microgrid system contains one renewable generator (wind turbine), one storage device (battery), and one local consumer. The microgrid system is connected to the external power grid through a transformer. All the components are characterized by the dynamic models, constraints, and reference profiles presented in the following.

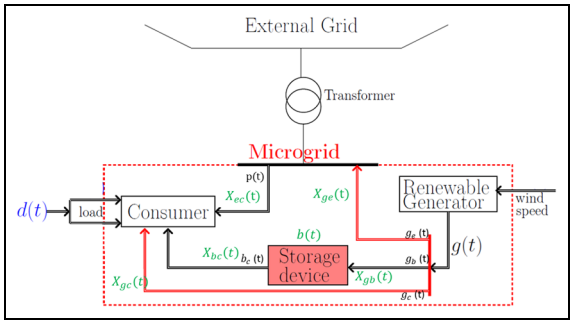

Figure 1. Microgrid.

The nature of this article is methodological and the considered system is a simplified example to illustrate the methods proposed. It is a system including a variety of components that make up a microgrid and define its characteristics. Other components, links, profiles and constraints can be added and modeled. Then, the optimization problem for the MPC can be regarded as a mixed-integer linear programming, for which various efficient solvers exist.

The microgrid can be modeled as a graph of four nodes (the external grid, the renewable generator, the battery and the consumer) and five links (from external grid to consumer, generator to external grid, generator to consumer, generator to battery and battery to consumer). In this work, the node representing the battery and the five links are considered dynamic.

Dynamic model of the microgrid. We consider the dynamic models for six components including the five links and the storage device (battery). The description of the system dynamics leads to a six-element state vector: five states contain the values of energy in the links that can propagate to the next node and the sixth represents the battery energy level[11]

$$\mathbf{x}(t) = \left[x_{ec}(t) x_{ge}(t) x_{gc}(t) x_{gb}(t) x_{bc}(t) b(t)\right]^T$$

The corresponding dynamic models are

External grid to consumer

$$x_{ec}(t+1) = (1-\alpha)x_{ec}(t) + \alpha p(t) \tag{16}$$

Generator to external grid

$$x_{ge}(t+1) = (1-\alpha)x_{ge}(t) + \alpha g_e(t) \tag{17}$$

Generator to consumer

$$x_{gc}(t+1) = (1-\alpha)x_{gc}(t) + \alpha g_c(t) \tag{18}$$

Generator to battery

$$x_{gb}(t+1) = (1-\alpha)x_{gb}(t) + \alpha g_b(t) \tag{19}$$

Battery to consumer

$$x_{bc}(t+1) = (1-\alpha)x_{bc}(t) + \alpha b_c(t) \tag{20}$$

where $\alpha \in [0,1]$ is a fixed constant, mainly dependent upon the size of the discretization step, and
Battery

$$b(t+1) = (1-\tau)b(t) + x_{gb}(t) - b_c(t) + w(t) \tag{21}$$

with the mixed-integer conditions[24]

$$\begin{cases} 0 \leqslant b_c(t) \leqslant Ma(t) \\ 0 \leqslant x_{gb}(t) \leqslant M(1-a(t)) \end{cases} \tag{22}$$

The above six state variables can be inferred by the vector of system control inputs $\mathbf{u}(t)$: $\mathbf{u}(t) = [p(t)g_e(t)g_c(t)g_b(t)b_c(t)]^T$ where[11]

- $p(t) \in \mathbb{R}$ (W) represents the electrical power transmitted by the external grid to the consumer at time step t.
- $g_e(t) \in \mathbb{R}$ (W) represents the electrical power transmitted by the renewable generator to the external grid at time step t.
- $g_b(t) \in \mathbb{R}$ (W) represents the electrical power transmitted by the renewable generator to the battery at time step t.
- $g_c(t) \in \mathbb{R}$ (W) represents the electrical power transmitted by the renewable generator to the consumer at time step t.
- $b_c(t) \in \mathbb{R}$ (W) represents the electrical power transmitted by the battery to the consumer at time step t.

The consumer has the possibility to take electrical power from the external grid, the renewable generator, and the battery. Thus, the sum of powers received by the consumer is $x_{ec}(t) + x_{gc}(t) + x_{bc}(t)$. Finally, the system output $y(t)$ is the total power received by the consumer

$$y(t) = x_{ec}(t) + x_{gc}(t) + x_{bc}(t)$$

In the end, the microgrid can be described by the following global dynamic model

$$\begin{aligned} \mathbf{x}(t+1) &= \mathbf{A}\mathbf{x}(t) + \mathbf{B}\mathbf{u}(t) \\ \mathbf{y}(t) &= \mathbf{C}\mathbf{x}(t) \end{aligned} \tag{23}$$

where

$$\mathbf{A} = \begin{bmatrix} 1-\alpha & 0 & 0 & 0 & 0 & 0 \\ 0 & 1-\alpha & 0 & 0 & 0 & 0 \\ 0 & 0 & 1-\alpha & 0 & 0 & 0 \\ 0 & 0 & 0 & 1-\alpha & 0 & 0 \\ 0 & 0 & 0 & 0 & 1-\alpha & 0 \\ 0 & 0 & 0 & 1 & 0 & 1-\tau \end{bmatrix}$$

$$\mathbf{B} = \begin{bmatrix} \alpha & 0 & 0 & 0 & 0 \\ 0 & \alpha & 0 & 0 & 0 \\ 0 & 0 & \alpha & 0 & 0 \\ 0 & 0 & 0 & \alpha & 0 \\ 0 & 0 & 0 & 0 & \alpha \\ 0 & 0 & 0 & 0 & 1 \end{bmatrix}$$

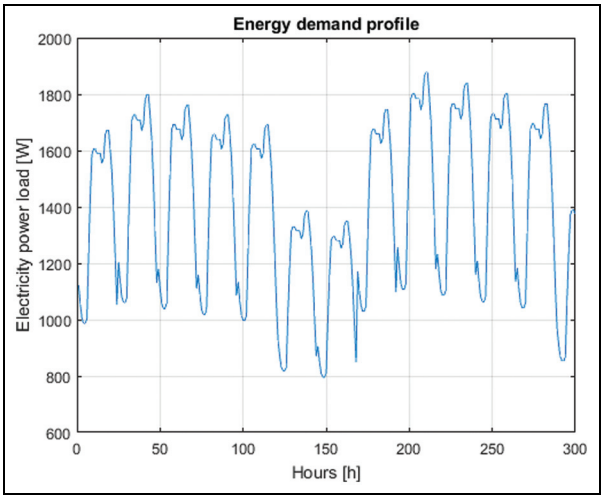

Figure 2. Consumer load profile.

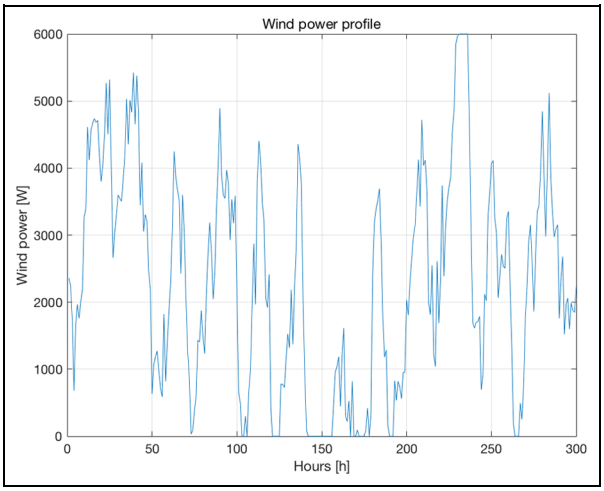

Figure 3. Wind power profile.

$$\mathbf{C} = [1 \quad 0 \quad 1 \quad 0 \quad 1 \quad 0]$$

Reference profiles. We consider two reference profiles characterizing the microgrid components (i.e. the consumer and the renewable generator) based on real numerical data taken from Grigg et al.,[33] and the details can be found in Prodan and Zio.[17] The consumer load takes into account seasonal numerical data and is predicted using weekly, daily, and hourly peaks. Figure 2 shows the consumer load profile $d(t) \in \mathbb{R}$. The wind speed used to calculate the wind power profile is estimated based on meteorological data. Figure 3 shows the power generator profile: the electrical power generated $g(t) \in \mathbb{R}$ is obtained from the wind speed profile.[34]

Optimization problem of the microgrid. The optimization problem is to find the appropriate control inputs that minimize the difference between the power demanded by the consumer and that actually received. Thus, the objective function for MPC is

$$\min_{[\mathbf{u}(t)]_{t=k:k+N_p}} \sum_{t=k}^{k+N_p} d(t) - y(t)$$

with the set of constraints defined in the following equations (24)–(28).

- Satisfaction of consumer power demands

$$0 \leqslant x_{ec}(t) + x_{gc}(t) + x_{bc}(t) \leqslant d(t) \tag{24}$$

where $d(t)$ is the consumer's demand.

- Battery storage

Batteries have their physical characteristics: the minimum-capacity B_{min} determined by the Depth of Discharge (DoD)[35] and the capacity B_{max}. The rate of the battery charge is also limited by some bounds

$$B_{min} \leqslant b(t) \leqslant B_{max} \tag{25}$$

$$Br_{min} \leqslant \Delta b(t) \leqslant Br_{max} \tag{26}$$

where $B_{min} \in \mathbb{R},\ B_{max} \in \mathbb{R},\ Br_{min} \in \mathbb{R},\ Br_{max} \in \mathbb{R}$.

- Generator

The power taken from the generator by the battery ($g_b(t)$), the consumer ($g_c(t)$) and the external grid ($g_e(t)$) is bounded by the power generated

$$0 \leqslant g_b(t) + g_c(t) + g_e(t) \leqslant g(t) \tag{27}$$

with $g_b(t) \geqslant 0,\ g_c(t) \geqslant 0,\ g_e(t) \geqslant 0$.

- Link capacities

$$\mathbf{u}_{min} \leqslant \mathbf{u}(t) \leqslant \mathbf{u}_{max} \tag{28}$$

where $u(t) \in \mathbb{R}$.

The numerical values of the parameters used for the simulations are taken from Grigg et al.[33] (see Table 1).

Table 1. Numerical data for the microgrid components.

Battery parameters	
τ	1.3×10^{-4}
M	9×10^{3}
B_{min}(W h)	1.2×10^{3}
B_{max}(W h)	9×10^{3}
Br_{min}(W)	-1.5×10^{3}
Br_{max}(W)	1.5×10^{3}
Control input constraints	
U_{min}	$[0\ \ 0\ \ 0\ \ 0\ \ 0]^T$
U_{max}	$[2\ \ 1.5\ \ 2\ \ 1.5\ \ 2]^T\times10^{3}$
Prediction horizon	
N_p	7
Simulation steps	
N	300

Scenarios

We consider two operation modes for the microgrid: grid-connected and stand-alone. Under these two modes, the microgrid is designed to satisfy consumers' demand. We assume that the external grid and the renewable generator are fault free. Then, threats to the microgrid service may come from failure of the links from the three sources (i.e. the external grid e_c, the renewable generator g_c, and the battery b_c) to the consumer. The two other links from the renewable generator (i.e. g_e and g_b) are also considered since they impact on the cost of the microgrid. The link failures are represented as the removal of the links and no recovery action is taken.

Grid-connected mode. During the grid-connected mode, the consumer takes electrical power from two sources: the external grid and the renewable generator.

The scenarios considered are the following:

- Scenario 1.0: the nominal functioning case, that is, fault free.
- Scenario 1.1: the link from the generator to the external grid is disconnected (i.e. g_e is removed).
- Scenario 1.2: the link from the generator to the consumer is disconnected (i.e. g_c is removed).

Note that the failure of the battery is not considered for the grid-connected mode, since in that mode it is assumed that the battery is not used.

Stand-alone mode. In stand-alone mode, the microgrid is disconnected from the external power grid and generation should by itself satisfy consumers' demand.

The scenarios considered are as follows:

- Scenario 2.0: the stand-alone functioning case (i.e. only p is disconnected).
- Scenario 2.1: the link from the generator to the consumer is disconnected (i.e. g_c is removed).
- Scenario 2.2: the link from the generator to the battery is disconnected (i.e. g_b is removed).
- Scenario 2.3: the link from the battery to the consumer is removed (i.e. b_c is removed)

Analysis of the results

We analyze the system property indexes introduced in section "System property indexes" for the scenarios described above. For the grid-connected mode, we also analyze the difference between cost and profit of the microgrid for each scenario. The simulation of each scenario is considered for the period of 300 h, during which the microgrid experiences almost all extreme conditions of consumer demands and wind power. The simulation is taken for the period of 300 h.

Grid-connected mode. From Table 2, we can see that in grid-connected mode, the demands of the consumers

Table 2. Index values for the grid-connected mode.

Scenario	*NSD*	*CI*	EI^{st}	Profit
1.0	0	1	1	+203.2
1.1	0	0.83	1	−77.0
1.2	0	0.83	1	−79.2

Table 3. Index values for the stand-alone mode.

Scenario	*NSD*	*CI*	EI^{st}
2.0	0.1065	0.83	0.667
2.1	0.6562	0.83	0.583
2.2	0.4190	0.83	0.667
2.3	0.4364	0.83	0.333

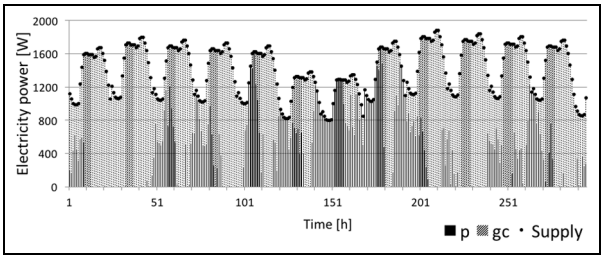

Figure 4. Supply sources of Scenario 1.0. The black area represents the power from the external grid and the shaded area represents the power from the renewable generator.

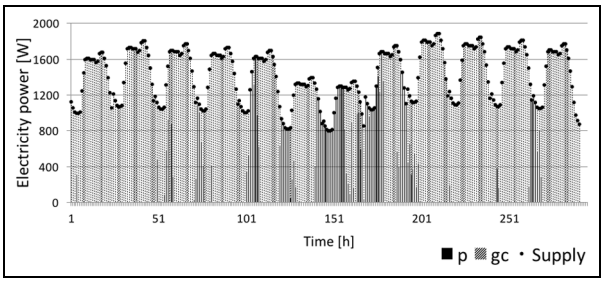

Figure 5. Supply sources of Scenario 1.1. The black area represents the power from the external grid and the shaded area represents the power from the renewable generator.

can always be satisfied. The two links have identical influence on the system controllability: with the removal of each link, the microgrid is no longer controllable, and the rank of controllability matrix decreases by 1, which means that one component is out of control. The capacity efficiency index, EI^{st}, remains the same for all the scenarios. However, the cost differs a lot: when the generator is able to provide power to the consumer and sell power to the external grid, the microgrid is profitable (Scenarios 1.0); otherwise, the microgrid spends money on electricity (Scenarios 1.1 and 1.2).

Figures 4 and 5 show the sources of the power actually received by the consumer for Scenario 1.0 and Scenario 1.1, respectively.

In Scenario 1.0, the consumer takes electrical power from the external grid and the renewable generator. We can see from Figure 4 that the renewable generator (g_c) provides most of the demanded power (represented by the shaded bar). If compared with the load profile and wind power profile (see Figure 2 and Figure 3), we can see that the consumer takes electricity from the external grid when the wind power is low; and when the wind power is high, the microgrid sells electricity to the external grid: this is why in the case of nominal functioning, the microgrid can make a profit.

In Scenario 1.1, the power sources remain the same as Scenario 1.0. The system properties remain the same as the nominal functioning case, and the sources of the supply to the consumer are almost the same as in Scenario 1.0 (see Figure 5). However, with the disconnection of the link g_e, it is impossible to sell electricity to recompense the expenses on electricity bought from the external grid; therefore, instead of making a profit, it spends money to buy electricity.

As for Scenario 1.2, where the link from the generator to the consumer g_c is disconnected, the consumer is supplied completely by the external grid, which also explains the fact that *NSD* is always equal to 0. In addition, since the capacity of link g_e is limited, the wind power generated cannot be fully sold, that is, the profit by selling electricity is not able to compensate the expenses.

In the grid-connected mode, the consumer's demand is always satisfied, which is natural and reasonable. However, the introduction of the microgrid (renewable generator) decreases the cost on electricity or even makes a profit, and it is, thus, interesting for economic considerations.

Stand-alone mode. From Table 3, we can see that the *NSD* increases in this mode and the demands are never fully satisfied. More detailed analysis is given in the following. The capacity efficiency index EI^{st} decreases, because the disconnection of the link p reduces the transmission capacity of the microgrid; this also contributes to the inadequate supply of the consumer's demands.

Figure 6 shows the sources of the power actually received by the consumer for Scenario 2.0. From the beginning to $t = 145$ h under this scenario, the supply is similar to that of Scenarios 1.0 and 1.1: the renewable generator provides most of the demanded power and the battery fills the unsatisfied portion, except for certain periods of low wind power generation. Then, the microgrid arrives at a relatively long period when there is no wind power at all, the battery reaches its lower limit and the supply is totally cut. Around $t = 200$ h, when the wind comes back to its usual level, the microgrid continues to function.

In Scenario 2.1, the control input of the link from the generator to the consumer g_c is lost, while the battery provides power to the consumer and can be

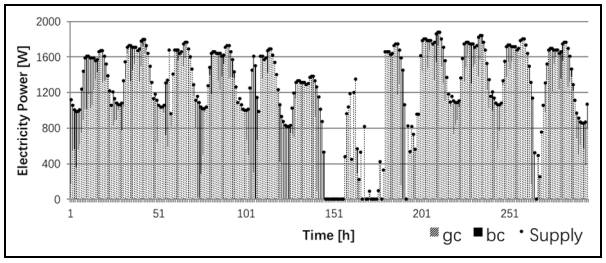

Figure 6. Supply sources of Scenario 2.0. The black area represents the power from the external grid and the shaded area represents the power from the renewable generator.

charged by g_b. *NSD* is the highest of all the stand-alone modes. This is due to the fact that the supply to the consumer is dominated by the capacity of the link from the battery (g_b has smaller capacity than g_b), which is also reflected by the fact that EI^{st} is lower than that of Scenario 2.0. In addition, when the battery reaches its lower limits and switches to charge mode, there is no supply to the consumer.

In Scenario 2.2, the link from the generator to the battery g_b is removed, that is, the battery can no longer be charged. The battery can provide part of the demanded power in the beginning and when the battery reaches its lower limit at $t = 20$ h, the renewable generator becomes the only source of supply to the consumer. *NSD* is much higher than that of Scenario 2.0. The consumer's demand can be satisfied only when there is enough wind power. During the period of high wind speed (the power generated can reach 6 kW, which is much higher than the largest demand), the redundant power generated cannot be stored. The capacity efficiency index EI^{st} is the same as Scenario 2.0 since the failed link does not affect the supply to the consumer; however, without it, the battery does not have income any more, which decreases the supply.

In Scenario 2.3, the link from the battery to the consumer b_c is failed, and the renewable generator is the only source to supply the consumer for the whole period. Under this scenario, *NSD* is similar to Scenario 2.2; but, without the contribution of the energy stored in the battery, *NSD* is slightly higher. In addition, the capacity efficiency is the lowest for Scenario 2.3 since there is only one source-terminal path left, that is, the link from the generator to the consumer.

In the stand-alone mode, we have $NSD > 0$ for all the scenarios considered. But, because of the integration of the renewable generator, a large part of the demand can be supplied. Furthermore, the importance of the storage device is shown through the comparison of the Scenarios 2.0, 2.2 and 2.3.

Conclusion

In this article, we have adopted MPC for describing microgrid dynamics and analyzed system performance under grid-connected and stand-alone modes for different failure scenarios. This analysis enables quantitative evaluation of microgrid performance with respect to different perspectives of reliability, controllability and topology.

We have considered a specific case study, which confirms the fact that the microgrid be connected to the external power grid is important to ensure supply to the consumer under different failure scenarios and that the introduction of microgrids composed of renewable generators and storage devices improves reliable performance of the power grid. The instability of the wind power and the limited capacity of the battery or links can be a barrier to the reliable service of the microgrid, especially when in stand-alone mode.

The findings of analyses of this kind provide information for the design and operation of the microgrid, seeking the right balance of multiple characteristics and least cost for the safe and reliable functioning of the microgrid system.

Declaration of Conflicting Interests

The author(s) declared no potential conflicts of interest with respect to the research, authorship, and/or publication of this article.

Funding

The author(s) received no financial support for the research, authorship, and/or publication of this article.

References

1. Kröger W and Zio E. *Vulnerable systems*. London: Springer-Verlag, 2011.
2. Rouse WB. Engineering complex systems: implications for research in systems engineering. *IEEE T Syst Man Cy C* 2003; 2(33): 154–156.
3. Ottino JM. Engineering complex systems. *Nature* 2004; 427(6973): 399.
4. Zio E. Challenges in the vulnerability and risk analysis of critical infrastructures. *Reliab Eng Syst Safe* 2016; 152: 137–150.
5. Zio E. Reliability analysis of systems of systems. *IEEE Reliability Magazine*, February 2016, pp.1–6.
6. Zio E. Critical infrastructures vulnerability and risk analysis. *Eur J Secur Res* 2016; 1: 97–114.
7. Zio E and Golea LR. Analyzing the topological, electrical and reliability characteristics of a power transmission system for identifying its critical elements. *Reliab Eng Syst Safe* 2012; 101: 67–74.
8. Li J, Dueñas-Osorio L, Chen C, et al. Connectivity reliability and topological controllability of infrastructure networks: A comparative assessment. *Reliab Eng Syst Safe* 2016, 156: 24-33.
9. Zhang L, Li D, Qin P, et al. Reliability analysis of interdependent lattices. *Physica A* 2016; 452: 120–125.
10. Lasseter RH and Paigi P. Microgrid: a conceptual solution. In: *2004 IEEE 35th annual power electronics specialists conference (PESC '04)*, Aachen, 20–25 June 2004, pp.4285–4290. New York: IEEE.

11. Han F, Prodan I and Zio E. A framework of model predictive control for the safety analysis of an electric power microgrid. In: *ESREL 2015, 25th European safety and reliability conference*, Zurich, 7–10 September 2015. London: CRC Press.
12. Zamora R and Srivastava AK. Controls for microgrids with storage: review, challenges, and research needs. *Renew Sustain Energ Rev* 2009; 147: 2009–2018.
13. Jimeno J, Anduaga J, Oyarzabal J, et al. Architecture of a microgrid energy management system. *Eur T Electr Power* 2011; 21(2): 1142–1158.
14. Kuznetsova E, Culver K and Zio E. Complexity and vulnerability of Smartgrid systems. In: *Proceedings of the European safety and reliability conference*, Troyes, pp.2474–2482. London: CRC Press.
15. Krause T, Beck EV, Cherkaoui R, et al. A comparison of Nash equilibria analysis and agent-based modelling for power markets. *Int J Elec Power* 2006; 28(9): 599–607.
16. Weidlich A and Veit D. A critical survey of agent-based wholesale electricity market models. *Energ Econ* 2008; 30(4): 1728–1759.
17. Prodan I and Zio E. A model predictive control framework for reliable microgrid energy management. *Int J Elec Power* 2014; 61: 399–409.
18. Prodan I and Zio E. On the microgrid energy management under a predictive control framework. In: *IEEE conference on control applications (CCA)*, Juan Les Antibes, 8–10 October 2014, pp.861–866. New York: IEEE.
19. Olivares DE, Mehrizi-Sani A, Etemadi AH, et al. Trends in microgrid control. *IEEE T Smart Grid* 2014; 5(4): 1905–1919.
20. Wang S, Li Z, Wu L, et al. New metrics for assessing the reliability and economics of microgrids in distribution system. *IEEE T Power Syst* 2013; 28(3): 2852–2861.
21. Rawlings JB and Mayne DQ. *Postface to model predictive control: theory and design*, 2011. USA: Nob Hill Publishing.
22. Richalet J and O'donovan D. *Predictive functional control: principles and industrial applications*. London: Springer-Verlag, 2009.
23. Goodwin GC, Seron M and De Dona J. *Constrained control and estimation: an optimisation approach*. London: Springer-Verlag, 2005.
24. Hovgaard TG, Larsen LF and Jorgensen JB. Robust economic MPC for a power management scenario with uncertainties. In: *Proceedings of the 50th IEEE conference on decision and control and European control conference (CDC-ECC)*, Orlando, FL, 12–15 December 2011, pp.1515–1520. New York: IEEE.
25. Halvgaard R, Poulsen NK, Madsen H, et al. Economic model predictive control for building climate control in a smart grid. In: *IEEE PES innovative smart grid technologies (ISGT)*, Washington, DC, 16–20 January 2012, pp.1–6. New York: IEEE.
26. Edlund K, Bendtsen JD and Jørgensen JB. Hierarchical model-based predictive control of a power plant portfolio. *Control Eng Pract* 2011; 19(10): 1126–1136.
27. Negenborn RR, De Schutter B and Hellendoorn H. Multi-agent model predictive control of transportation networks. In: *Proceedings of the IEEE international conference on networking, sensing and control*, Fort Lauderdale, FL, 23–25 April 2006, pp.296–301. New York: IEEE.
28. Fang Y and Zio E. Hierarchical modeling by recursive unsupervised spectral clustering and network extended importance measures to analyze the reliability characteristics of complex network systems. *Am J Oper Res* 2013; 3(1A): 101–112.
29. Lombardi A and Hörnquist M. Controllability analysis of networks. *Phys Rev E* 2007; 75: 056110.
30. Liu YY, Slotine JJ and Barabási AL. Controllability of complex networks. *Nature* 2011; 473: 167–173.
31. Bakolas A and Saleh JH. Augmenting defense-in-depth with the concepts of observability and diagnosability from control theory and discrete event systems. *Reliab Eng Syst Safe* 2011; 96(1): 184–193.
32. Kalman RE. Mathematical description of linear dynamical systems. *J Soc Ind Appl Math* 1963; 1(2): 152–192.
33. Grigg C, Wong P, Albrecht P, et al. The IEEE reliability test system-1996. A report prepared by the reliability test system task force of the application of probability methods subcommittee. *IEEE T Power Syst* 1999; 143: 1010–1020.
34. Justus CG, Hargraves WR and Yalcin A. Nationwide assessment of potential output from wind-powered generators. *J Appl Meteorol* 1976; 15(7): 673–678.
35. Prodan I, Zio E and Stoican F. Fault tolerant predictive control design for reliable microgrid energy management under uncertainties. *Energy* 2015; 91: 20–34.